AD-A115 947 CASE WESTERN RESERVE UNIV CLEVELAND OH DEPT OF METAL--ETC F/G 11/2
OXIDATION OF NON-OXIDE CERAMICS.(U)
MAY 82 T E MITCHELL, A H HEUER F49620-78-C-0053
UNCLASSIFIED AFOSR-TR-82-0482 NL

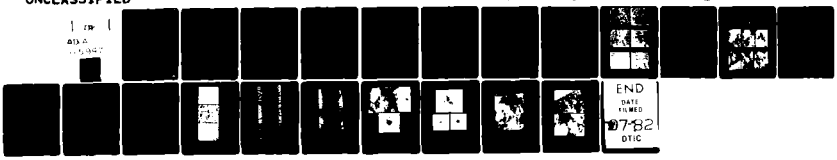

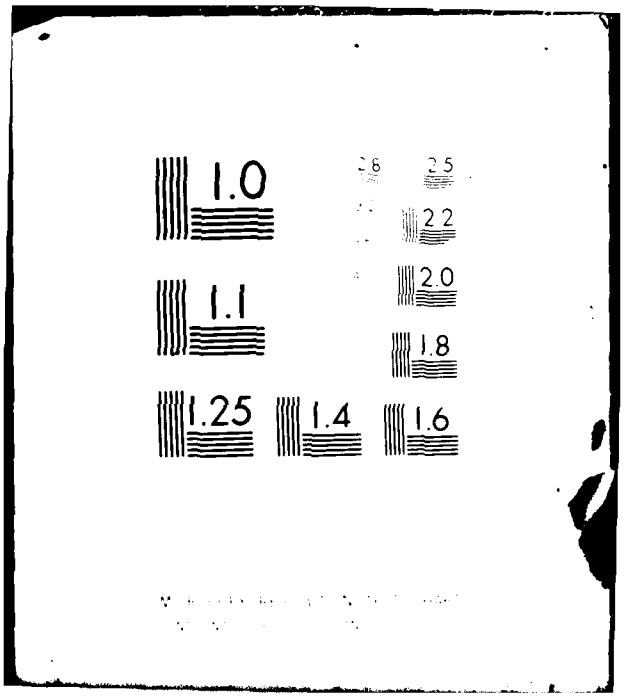
1.0
2.8
2.5
2.2
2.0
1.1
1.8
1.25
1.4
1.6

UNCLASSIFIED

SECURITY CLASSIFICATION OF THIS PAGE (When Data Entered)

(12)

AD A115947

REPORT DOCUMENTATION PAGE		READ INSTRUCTIONS BEFORE COMPLETING FORM
1. REPORT NUMBER AFOSR-TR- 82-0482	2. GOVT ACCESSION NO.	3. RECIPIENT'S CATALOG NUMBER
4. TITLE (and Subtitle) OXIDATION OF NON-OXIDE CERAMICS		5. TYPE OF REPORT & PERIOD COVERED FINAL FEB 75 - FEB 82
		6. PERFORMING ORG. REPORT NUMBER
7. AUTHOR(s) T. E. Mitchell and A. H. Heuer		8. CONTRACT OR GRANT NUMBER(s) F49620-78-C-0053
9. PERFORMING ORGANIZATION NAME AND ADDRESS Case Western Reserve University Cleveland, Ohio 44106		10. PROGRAM ELEMENT, PROJECT, TASK AREA & WORK UNIT NUMBERS 61102F 2305/A1
11. CONTROLLING OFFICE NAME AND ADDRESS AFOSR/NE Bolling Air Force Base - Bldg. 410 Washington, D.C. 20332		12. REPORT DATE 25 MAY 82
		13. NUMBER OF PAGES 18
14. MONITORING AGENCY NAME & ADDRESS (if different from Controlling Office)		15. SECURITY CLASS. (of this report) UNCLASSIFIED
		15a. DECLASSIFICATION DOWNGRADING SCHEDULE

16. DISTRIBUTION STATEMENT (of this Report)

Approved for public release;
distribution unlimited.

17. DISTRIBUTION STATEMENT (of the abstract entered in Block 20, if different from Report)

18. SUPPLEMENTARY NOTES

19. KEY WORDS (Continue on reverse side if necessary and identify by block number)

Oxidation, silcon carbide, silicon nitride

20. ABSTRACT (Continue on reverse side if necessary and identify by block number)

Oxidation mechanisms of SiC were determined. It was found that crestobalite nucleates at the SiC/SiO2 interface with appreciable heterogeneous nucleation during the first hour. Identical oxidation mechanisms were found for both single crystal and sintered polycrystalline SiC. Oxidation of yttria stabilized silicon nitride was investigated to determine the cause of the catastrophic oxidation at 1000C. At high temperature, SiO2 covers the entire surface, but at low temperature it does not. This allows the unstable yttria silicon oxynitride phases to form and cause catastrophic failure. No evidence of the effect of tungsten was noted.

UNCLASSIFIED

SECURITY CLASSIFICATION OF THIS PAGE (When Data Entered)

AFOSR-TR- 82-0482

Final Scientific Report On

OXIDIATION OF NON-OXIDE CERAMICS

submitted to the Air Force Office of Scientific Research

Contract No. F49620-78-C-0053

for the period February,1975 - February,1982

by

T. E. Mitchell and A. H. Heuer

Department of Metallurgy and Materials Science
Case Western Reserve University
Cleveland, Ohio 44106

April 1982

1. Introduction

This report describes the progress and publications which have resulted from AFOSR support of our research on tran_formation, oxidation and sintering of non-oxide ceramics, particularly silicon carbide and silicon nitride. This research has continued to be directed closely by Professors Heuer and Mitchell with the recent active research being performed by Ms. Mieskowski (for her M.S. thesis) and Dr. K. Kuroda. In addition, we have enjoyed stimulating collaboration with Prof. Cannon (MIT), Prof. Moller (Gottingen) and Dr. Tighe (NBS). The results of this research are described below and in the various Appendices. Section 5 lists our recent publications deriving from AFOSR sponship. Our earlier work with Drs. Lou, Ogbuji and Shinozaki on the $\beta \rightarrow \alpha$ transformation in SiC and on grain boundary phases in Si_3N_4 are given in References 1-9.

2. Oxidation of SiC

All research was conducted on single crystals (high and low purity) and sintered polycrystalline SiC (α and β) in the temperature range 1200-1400°C and in air and oxygen environments. Optical, scanning electron and transmission electron microscopy were used to examine the oxide film. Experiments showed that cristobalite nucleates at the SiC/SiO_2 interface, and also that appreciable heterogeneous nucleation occurs during the first hour of oxidation. The growth rate of cristobalite was determined to be linear until the point where impingement of the cristobalite spherulites occurred. Nucleation and growth rates of cristobalite appeared to be the same for both single crystals and sintered polycrystalline SiC. This is not surprising considering the low additive and impurity content of sintered polycrystalline SiC.

Oxidation kinetics were estimated from film thickness measurements (based on interference colors produced by the SiO_2 film) from sintered polycrystalline SiC and were found to be the same for the α and β polytypes. These values are noted in the table on the next page.

Temp. (°C)	k_p in O_2 (nm^2/min)
1200	2.4×10^2
1300	3.9×10^2
1400	7.1×10^2

These are typical values for the oxidation of SiC and give an activation energy of ∿113kJ/mole. The parabolic rate constant, k_p, for the oxidation of SiC single crystals at 1350°C in O_2 was found to lie between the values noted above for 1300°C and 1400°C, indicating identical oxidation mechanisms for both single crystal and sintered polycrystalline SiC.

More details of this research are provided in the attached paper (14) (Appendix 1 - to be published in the Proceedings of the Electron Microscopy Society of America) and in the M.S. Thesis of Ms. Diane Mieskowski. At least one additional paper will be forthcoming.

3. Oxidation of Silicon Nitride

Some compositions of Y_2O_3-doped Si_3N_4 are unstable at low temperatures (∿1000°C) during oxidation while they are passive at high temperatures (∿1400°C). This has been investigated by various analytical electron microscope techniques. At high temperatures, SiO_2 initially forms over the entire surface, following which the β-$Y_2Si_2O_7$ phase nucleates and grows as needles within the SiO_2 phase; the oxide layer remains protective. At low temperatures, it appears that the SiO_2 phase does not provide sufficient coverage and that various unstable phases (yttrium silicon oxidynitrides and tungsten oxidation products) form and cause degradation. Details are provided in the attached papers. Appendix 2 is to be published in the 1982 EMSA Proceedings (15). Appendix 3 is the first draft of a manuscript (17).

4. Sintering of SiC. We have previously approached the controversial area of the sintering of covalent solids from a theoretical point of view, in particular the structure of grain boundaries (13) and pore configurations (16) during the stays of Profs. Moller and Cannon. We have continued to cooperate with Prof. Cannon on an experimental investigation of SiC densification during sintering. Specimens sintered with B and C additions were prepared at M.I.T. by Prof. Cannon and C. C. Cranmer and examined here using transmission electron microscopy. Powder compacts have been fired to less than full density so that phases forming during the early stages of sintering could be examined and analyzed. Specimen density and firing temperature are noted below. All heat treatments were performed in an Ar atmosphere for 1 hr periods.

Temp. (°C)	True Density (%)
1900	69.1
2000	93.5
2050	97.9
2100	96.2

The low density specimen fired at 1900°C has been particularly illuminating. An amorphous grain boundary phase is observed which is no longer detectable in the higher density specimen. Edax analysis failed to detect any elements with $Z \gtrsim 10$. In consequence the presence of light elements was investigated using EELS analysis at Argonne with the help of M. Zaluzec for the specimen fired at 1900°C. This revealed a C-rich phase in the pores and between grains. Additional experiments are underway to evaluate microstructures resulting from additions of C only, B only, and B_4C.

This research is also part of Ms. Mieskowski's M.S. thesis and will be published.

5. Publications

The following papers have resulted from AFOSR-sponsored research over the past few years:

1. A.H.Heuer, V.Lou and L. Ogbuji, "Lattice Resolution Studies of Engineering Ceramics: SiC and Si_3N_4", J. Microscop. Spectrosc. Elect., 2, 475 (1977).

2. V. Lou, D.G.Howitt, L.Ogbuji, D.S.Phillips, D.L.Porter, A.H.Heuer, L.W.Hobbs and T.E.Mitchell, "Application of High Resolution TEM to Ceramic Science", in "Developments in Electron Microscopy and Analysis 1977, D.L.Misell, ed., Inst. of Phys., London, p. 203 (1977).

3. A.H.Heuer, G.A.Fryburg, L.U.Ogbuji, S.Shinozaki and T.E.Mitchell, "The $\beta \rightarrow \alpha$ Transformation in SiC: I-Microstructural Aspects", J. Amer. Ceram. Soc., 61, 406 (1978).

4. T.E.Mitchell, L.U.Ogbuji and A.H.Heuer, "The $\beta \rightarrow \alpha$ Transformation in Polycrystalline SiC: II-Interfacial Energetics", J. Amer. Ceram Soc., 61, 413 (1978).

5. L.K.V.Lou, T.E.Mitchell and A.H.Heuer, "Impurity Phases in Hot-pressed Si_3N_4", J. Amer. Ceram. Soc., 61, 392 (1978).

6. L.K.V.Lou, T.E.Mitchell and A.H.Heuer, "Discussion of Grain Boundary Phases in a Hot-pressed MgO Fluxed Silicon Nitride", J. Amer. Ceram. Soc., 61, 462 (1978).

7. A. H. Heuer, L. U. Ogbuji and T. E. Mitchell, "High Resolution Studies of the Final Stages of the $\beta \rightarrow \alpha$ Transformation in Polycrystalline SiC" in "Electron Microscopy and Analysis 1979", (Inst. of Physics, London) p. 453 (1980).

8. L. U. Ogbuji, T. E. Mitchell and A. H. Heuer, "The $\beta \rightarrow \alpha$ Transformation in Polycrystalline SiC: III, The Thickening of α Plates", J. Amer. Ceram. Soc., 64, 91 (1981).

9. L. U. Ogbuji, T. E. Mitchell, A. H. Heuer and S. Shinozaki, "The Transformation in Polycrystalline SiC: IV, A Comparison of Conventionally Sintered, Hot-Pressed, Reaction-Sintered and Chemically Vapor-Deposited Samples", J. Amer. Ceram. Soc., 64, 100 (1981).

10. A. H. Heuer, L. U.Ogbuji and T. E. Mitchell, "The Microstructure of Oxide Scales on Oxidized Si and SiC Crystals", J. Amer. Ceram. Soc., 63, 354 (1980).

11. N. J. Tighe, K. Kuroda, T. E. Mitchell and A. H. Heuer, "In Situ Oxidation of Y_2O_3-doped Si_3N_4" in Electron Microscopy 1980, Vol. 4, High Voltage, p. 310 (1980).

12. L. U. Ogbuji, T. E. Mitchell and A. H. Heuer, "Plastic Deformation During the Intermediate Stages of Sintering", in "Sintering Processes", edited by G. C. Kuczynski (Plenum Press), p. 135 (1980).

13. H. -J. Moller, " 011 Tilt Boundaries in the Diamond Cubic Lattice", Phil. Mag., 43, 1045 (1981).

14. D. M. Mieskowski, T. E. Mitchell and A. H. Heuer, "Microstructure of Oxide Films on SiC", in "Proceedings of Electron Microscopy Society of America", edited by G. W. Bailey (Claitors Press) (1982).

15. K. Kuroda, H. C. Liu, A. H. Heuer and T. E. Mitchell, "Microstructures of Oxidized Si_3N_4-8% Y_2O_3", in "Proceedings of Electron Microscopy Society of America", edited by G. W. Bailey (Claitors Press) (1982).

16. R. M. Cannon, "On the Effects of Dihedral Angle and Pressure on the Driving Forces for Pore Growth on Shrinkage", to be published.

17. K. Kuroda, A. H. Heuer and T. E. Mitchell, "Oxidation of Si_3N_4-8% Y_2O_3", see Appendix 3.

MICROSTRUCTURE OF OXIDE FILMS ON SiC

D. M. Mieskowski, T. E. Mitchell and A. H. Heuer

Department of Metallurgy and Materials Science
Case Western Reserve University, Cleveland, OH 44106

SiC is a ceramic which is used for abrasives and heating elements and has potential high temperature structural applications. Between 1200-1400° C, and at sufficiently high oxygen partial pressures, SiC develops a protective SiO_2 film. The film produced at short oxidation times (less than 5 hrs.) is mostly amorphous SiO_2 but becomes increasingly crystalline as oxidation continues. The crystalline phase is cristobalite which nucleates and grows as disc-shaped "spherulites" (1,2). The present paper describes a microstructural investigation of the SiO_2 film.

Figure 1 is an optical micrograph of a film formed on sintered alpha polycrystalline SiC at 1350° C. Because the film is transparent, spherulites can be seen at the SiO_2/SiC interface along with pits on the substrate surface and bubbles on the film surface. The spherulites range in size from 10-40μm in diameter and are limited in thickness by the film which is 0.25 μm thick. They nucleate at the film/substrate interface (1), are covered by a layer of amorphous SiO_2, and have arms which appear as needle-like rays. Spherulitic structure may be better seen in Figure 2 which is a scanning electron micrograph of a spherulite formed on a low purity SiC single crystal at 1350° C. It was exposed by dissolving the amorphous SiO_2 with a dilute solution of HF. Here the arms are contained within the spherulite disc, an observation not generally possible with optical microscopy because interference colors produced by film thickness variations often mask spherulites on polycrystalline SiC. The bright-field transmission electron micrograph (Figure 3) shows a spherulite formed on sintered alpha SiC at 1300° C. Twins and stacking faults are the dominant features as evidenced by extra spots and streaks in the diffraction pattern.

Bubbles form abundantly during the oxidation of sintered polycryatalline SiC but rarely during the oxidation of single crystals. This, apparently, is due to the oxidation of B_4C/C inclusions present in the polycrystalline material. Bubble formation is discussed with reference to Figures 4-6. Figure 4 is a scanning electron micrograph of an unoxidized sintered beta SiC surface. The dark spots are inclusions. That these inclusions form gaseous species during oxidation is indicated by Figure 5, a micrograph showing the SiC substrate after removal of the oxide. It is evident that the inclusions have been replaced by pits. During oxidation, SiO_2 forms over the SiC surrounding the inclusions and, when the film is sufficiently thick, flows onto the inclusions and covers them, resulting in bubbles such as are shown in Figure 6. These bubbles eventually burst and then heal, causing thickness variations in the film.

Both of these phenomena, crystallization and bubble formation, are expected to affect the oxidation kinetics. These kinetics are parabolic and result from the inward diffusion of oxygen to the film/substrate interface where it reacts to form SiO_2 and CO (1,3,4). Crystallization would increase oxidation by providing short-circuit paths for the diffusion of oxygen as would local reductions in film thickness due to bubble formation.

This research was supported by AFOSR Grant No. F49620-78C-0053.

1. J.A.Costello and R.E.Tressler, J. Amer. Cer. Soc., 64, 327 (1981).
2. L.U.Ogbuji, A.H.Heuer and T.E.Mitchell, J. Amer. Cer. Soc., 63, 354 (1980).
3. K.Motzfeldt, Acta Chem. Skand., 18, 1596 (1964).
4. J.Schlichting, Rev. Int. Hautes Temper. Refrac., 16, 67 (1979).

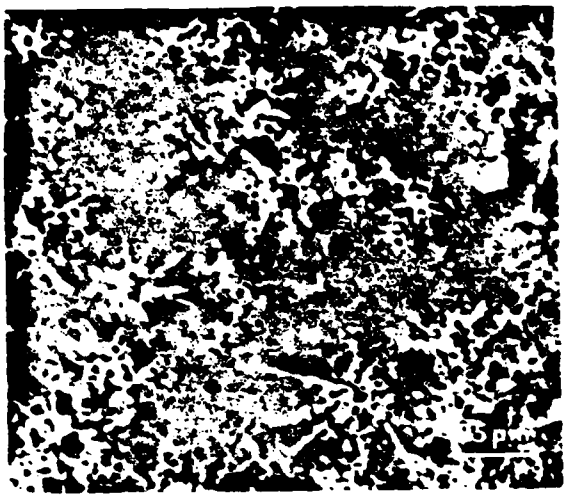

Fig. 1. Sintered alpha SiC oxidized at 1350° C in air (optical micrograph)

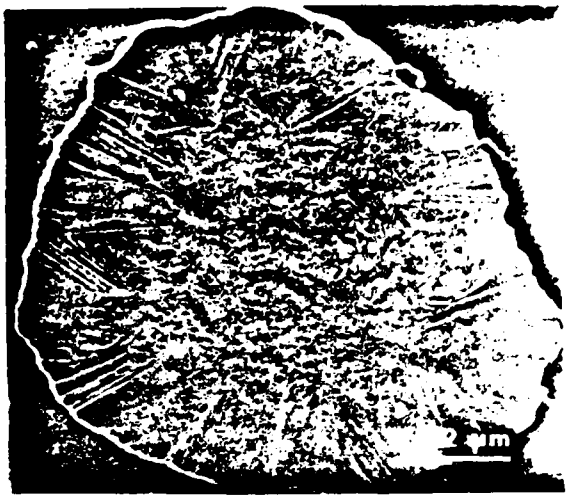

Fig. 2. Cristobalite spherulite on alpha SiC single crystal oxidized at 1350° C in O_2 (SEM)

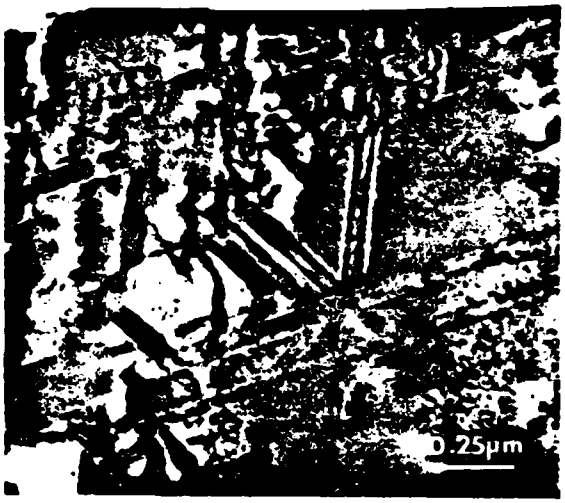

Fig. 3. Twins and stacking faults in cristobalite spherulite formed on sintered alpha SiC in O_2 at 1300° C (TEM)

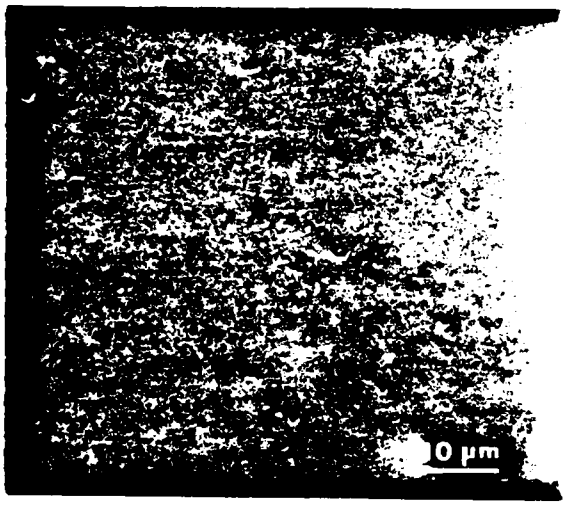

Fig. 4. Unoxidized polished surface of sintered beta SiC (SEM)

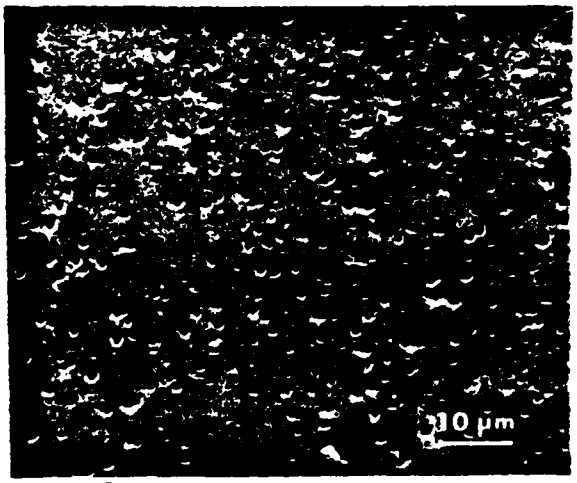

Fig. 5. Surface of sintered beta SiC after oxidation at 1400° C in O_2 and removal of oxide film (SEM)

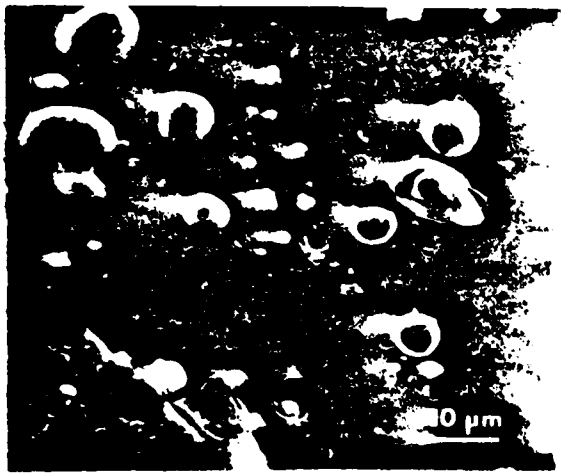

Fig. 6. Bubbles on oxide surface of sintered beta SiC (SEM)

MICROSTRUCTURES OF OXIDIZED Si_3N_4-8%Y_2O_3

K. Kuroda, H. C. Liu, A. H. Heuer and T. E. Mitchell

Department of Metallurgy and Materials Science
Case Western Reserve University, Cleveland, Ohio 44106

Introduction. There is considerable interest in the effect of oxidation on the microstructure of yttria-doped silicon nitride, since some compositions are unstable at low temperatures (≈1000°C) despite their apparent stability at 1400°C (1). The material used in this study was the same commercial hot-pressed Si_3N_4-8%Y_2O_3 (NCX-34) as one investigated previously (2), which had exhibited only passive oxidation during heating in air from 600° to 1400°C. Some thin (≈100μm) specimens were oxidized at 800°, 1000° and 1450°C in ambient air and then ion-thinned from one side; others were ion-milled and oxidized. Specimens were examined by scanning electron microscopy (SEM) and transmission electron microscopy (TEM) along with energy dispersive x-ray (EDX) analysis.

High temperature oxidation. Surface morphologies after oxidation at 1450°C are shown in the scanning electron micrograph in Fig. 1. Both needle-like structures and small particles coexist after 80 min oxidation, however, the needle-like structures became dominant after long-term oxidation. This implies that the needle-like structures form as a result of coalesence of homogeneously-nucleated particles. TEM micrographs (Fig. 2) show microstructures of the surface layer after 10 hr oxidation. Very dark regions in Fig. 2a, which correspond to the oxidation products in Fig. 1, are confirmed as β-$Y_2Si_2O_7$(3) by EDX and diffraction analysis. Fig. 2b shows a low angle grain-boundary and a stacking fault in the β-$Y_2Si_2O_7$ phase. Twins are also observed. The planar defects in the needle-like phase are probably interfaces produced by coalescense of nuclei. The other major phase near the surface after oxidation is β-SiO_2 cristobalite as shown in Fig. 2c, having almost identical grain size (1.2μm) with some subgrains and also microcracks. Grain-boundary phases are found to be amorphous from microdiffraction pattern. Porosity (arrowed in Fig. 2a) is thought to be in the tungsten phase which results from contamination from WC balls during ball-milling of the silicon nitride powder. EDX data indicates that the tungsten phase is not present near the oxidized surface after 72 hr oxidation.

Low temperature oxidation. SiO_2 and/or Si_2N_2O nuclei on β-Si_3N_4 grains are observed after 2 hr oxidation at 1000°C (Fig. 3a). The pre-existing yttria silicon oxynitride phase becomes porous after 2 hr oxidation and oxidation products form near the interface with β-Si_3N_4 (Fig. 3b). Cracks appear along some grain boundaries. These features are quite similar to the results of the in-situ experiments on the other billet from the same manufacturer, which exhibited catastrophic low temperature oxidation (2). Fig. 4 shows that SiO_2 forms on some β-Si_3N_4 grains after 20 hr oxidation. Further TEM observation, however, indicated that oxidation had not occurred uniformly over the specimen. Loss of W was not detected by EDX analysis after 20 hr oxidation at 1000°C.

This work was supported by AFOSR Contract No. F49620-78C00053.

References

1) F.F.Lange, S.C.Singhal and R.C.Kuznicki, J. Am. Ceram. Soc., 60 (1977),249.

2) N.J.Tighe, K.Kuroda, T.E.Mitchell and A.H.Heuer, Electron Microscopy 1980, Vol. IV, p. 310.

3) J.Ito and H.Johnson, Am. Mineral., 53 (1968), 1940.

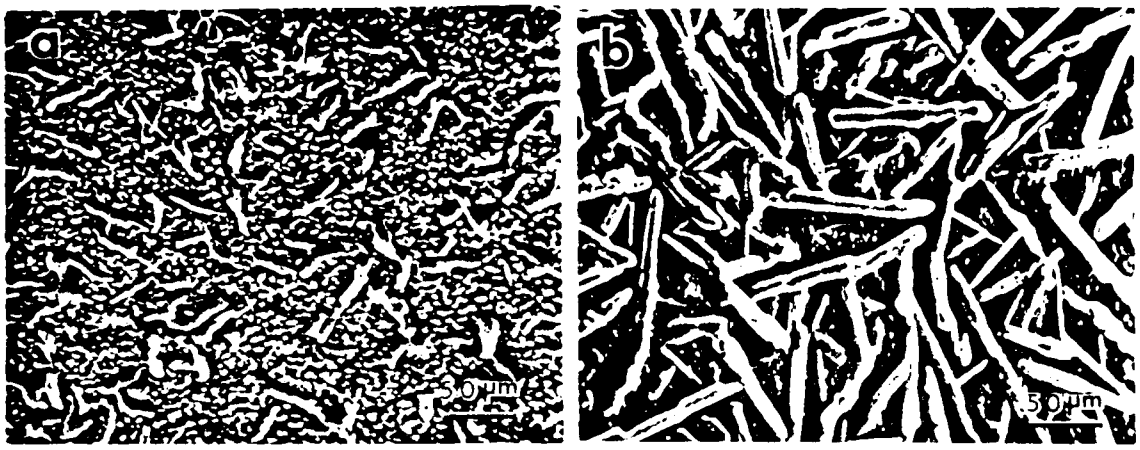

Fig. 1. SEM micrographs of Si_3N_4-8%Y_2O_3 oxidized at 1450°C for (a) 80 min and (b) 72 hr.

Fig. 2. TEM micrographs of back-thinned specimens oxidized at 1450°C for 10 hr.: (a) BF, (b) DF with β-$Y_2Si_2O_7$ reflection, (c) BF.

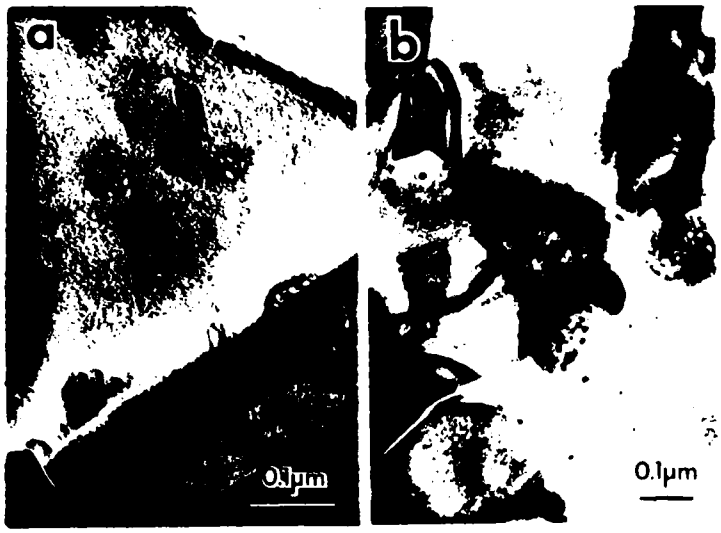

Fig. 3. BF TEM micrographs of specimens ion-milled and then oxidized at 1000°C for 2 hr.

Fig. 4. BF TEM micrograph of back-thinned specimen oxidized at 1000°C for 20 hr.

OXIDATION OF Si_3N_4-8% Y_2O_3

K. Kuroda, A. H. Heuer and T. E. Mitchell
Department of Metallurgy and Materials Science
Case Western Reserve University
Cleveland, Ohio 44106

1. Introduction

The oxidation of hot-pressed Si_3N_4 containing Y_2O_3 is technologically important because some compositions are unstable at low temperatures (≈1000°C) despite their apparent stability at high temperatures (≈1400°C). Lange et al. [1] discovered that $Si_3Y_2O_3N_4$ compounds showed a severe degradation at 1000°C. Weaver and Lucek [2] found that compositions containing the phase $Si_3Y_2O_3N_4$ were the ones that oxidized rapidly at 1000°C. Tighe et al. [3] observed catastrophic oxidation of Y_2O_3-doped Si_3N_4 in air at 740 C. In this project we have focussed on the effect of oxidation on the microstructure of Y_2O_3-doped Si_3N_4 in order to understand the changing oxidation resistance in the temperature range 800°to 1450°C.

2. Experimental procedures

The materials used in this study were the same commercial hot-pressed Si_3N_4-8% Y_2O_3 (NCX-34) as those investigated previously [3], which had exhibited only passive oxidation during heating in air from 600° to 1400°C. The major crystalline phases in the material were identified by powder x-ray diffraction as β-Si_3N_4, $Y_{10}Si_7O_{23}N_4$ (H phase) and WSi_2; however, there were some unidentified lines [3]. The tungsten phase (3-4%) results from tungsten carbide ball milling. Some thin (≈100 μm) specimens were oxidized at 800°, 1000° and 1450°C in ambient air and then ion-thinned from one side (back-thinned); others were ion-milled and then oxidized. Specimens were examined by scanning electron microscopy (SEM) and transmission electron microscopy (TEM) along with energy dispersive x-ray (EDX) analysis.

3. Results and Discussions

3.1 High Temperature Oxidation

Surface morphologies after oxidation at 1450°C are shown in Fig. 1. Both needle-like structures and small particles co-exist after 80 min oxidation; however, the needle-like structures become dominant after longer-term oxidation. EDX maps (Fig. 2) show that yttrium depletion occurs in the regions adjacent to the needle-like structures. These observations imply that the needle-like structures form as a result of coalesence of yttrium-phase particles which have nucleated in the surface oxide layer.

The TEM micrograph in Fig. 3a shows the microstructure of the surface layer after 10 hr oxidation. The very dark regions in Fig. 3a, which correspond to the yttria-phase in Fig. 1 and Fig. 2, are confirmed as β-$Y_2Si_2O_7$ [4] by EDX and diffraction analysis. This phase is also seen as light regions in the back scattered electron image in Fig. 3b. The other major phase near the surface after oxidation is cristobalite (SiO_2). Cracks are observed in the oxidized layer across the β-$Y_2Si_2O_7$ and SiO_2 phases. Presumably these cracks formed after oxidation during cooling to room temperature due to the difference in thermal expansion coefficients of two phases or due to the stress in the oxidized layer associated with oxidation. Porosity (arrowed in Fig. 3a) is thought to be in the tungsten phase. EDX data indicate that the tungsten phase is not present near the oxidized surface after 72 hr oxidation. The tungsten had apparently evaporated from the oxidized layer, probably as WO_3.

More detailed aspects of the β-$Y_2Si_2O_7$ phase are shown in Fig. 4. A low angle grain-boundary, a stacking fault (Fig. 4a) and a twin (Fig. 4b) are observed. The planar defects in the β-$Y_2Si_2O_7$ are probably interfaces produced by coalesence of nuclei. Fig. 4c is a convergent beam electron diffraction pattern from this phase showing the [100] zone axis.

Fig. 5a shows that cristobalite contains subgrains and also microcracks. Diffraction patterns indicate unambiguously that some of the SiO_2 is crystalline (Fig. 5b) but that the grain-boundary phase is non-crystalline (Fig. 5c), possibly as a result of the influence of additive or impurity elements.

From the microstructural observations, an oxidation mechanism can be proposed as follows: SiO_2 immediately forms over the entire surface at high temperatures (≈1450°C). The β-$Y_2Si_2O_7$ phase homogeneously nucleates in, and/or on, the SiO_2 layer and grows in the form of needle-like structures as a result of coalescence of nuclei.

3.2 Low Temperature Oxidation

Oxidation features were much the same at temperatures of 800° and 1000°C. TEM observations indicate that oxidation had not occurred uniformly over the specimen after 72 hr oxidation at 800 C. Fig. 6 shows that SiO_2 forms on some β-Si_3N_4 grains after 20 hr oxidation at 1000°C. The non-uniform oxidation is not surprising because weight gain data on NCX-34 [2] have shown that, at ≤1200°C, the total weight gain after 96 hr is only ≤0.07 mg/cm^2; however, at 1300°C, the weight gain is 0.2 mg/cm^2 after 100 hr. In order to examine the first oxide phase, specimens were ion-milled and then oxidized for short times. SiO_2 and/or Si_2N_2O nuclei on β-Si_3N_4 grains are observed after 2 hr oxidation at 1000°C. (Fig. 7a). Fig. 7b shows that the pre-existing yttria silicon oxynitride phase (H-phase) becomes porous and oxidation products form in this phase, which are too small to identify. Cracks appear along some grain boundaries.

The instability of Y_2O_3-doped hot-pressed Si_3N_4 at low temperatures can be explained by suggesting that the SiO_2 phase would be insufficient to cover entirely the surface since β-Si_3N_4 does not exhibit much oxidation. Therefore, the unstable phases could cause degradation or catastrophic oxidation at lower temperatures.

Our previous work indicated that the volatization of tungsten created voids on the other billet from the same manufacturer, which exhibited catastrophic low temperature oxidation [3]. However, the loss of tungsten in the present material was not detected by EDX analysis after 20 hr oxidation at 1000°C and void formation was not observed in the tungsten phase.

References

1. F.F.Lange, S.C.Singhal and R.C.Kuznicki, J. Am. Ceram. Soc., 60 (1977), 249.

2. G.Q.Weaver and J.W.Lucek, Ceramic Bull., 57 (1978), 1131.

3. N.J.Tighe, K.Kuroda, T.E.Mitchell and A.H.Heuer, Electron Microscopy 1980, Vol. IV, p. 310.

4. J.Ito and H.Johnson, Am. Mineral., 53 (1968), 1940.

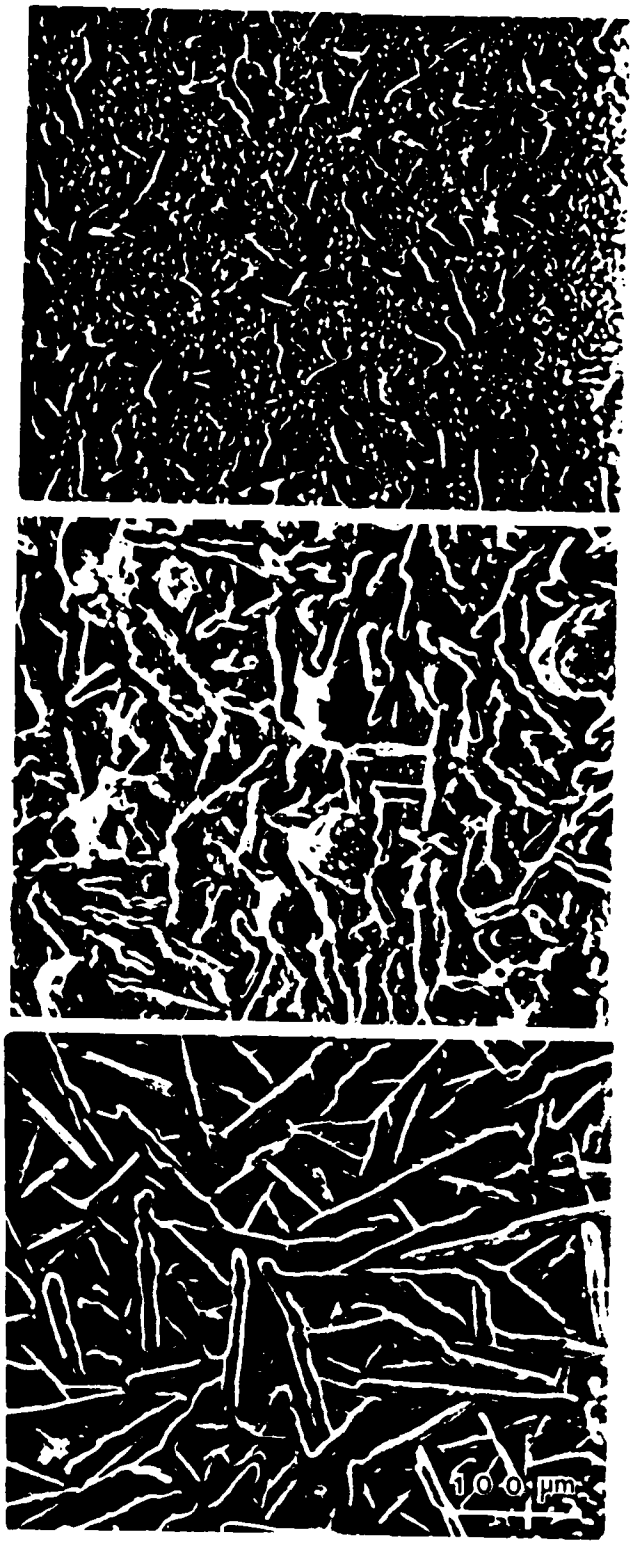

Fig. 1. SEM micrographs of Si_3N_4-8%Y_2O_3 oxidized at 1450°C for (a) 80 min, (b) 48 hr and (c) 72 hr.

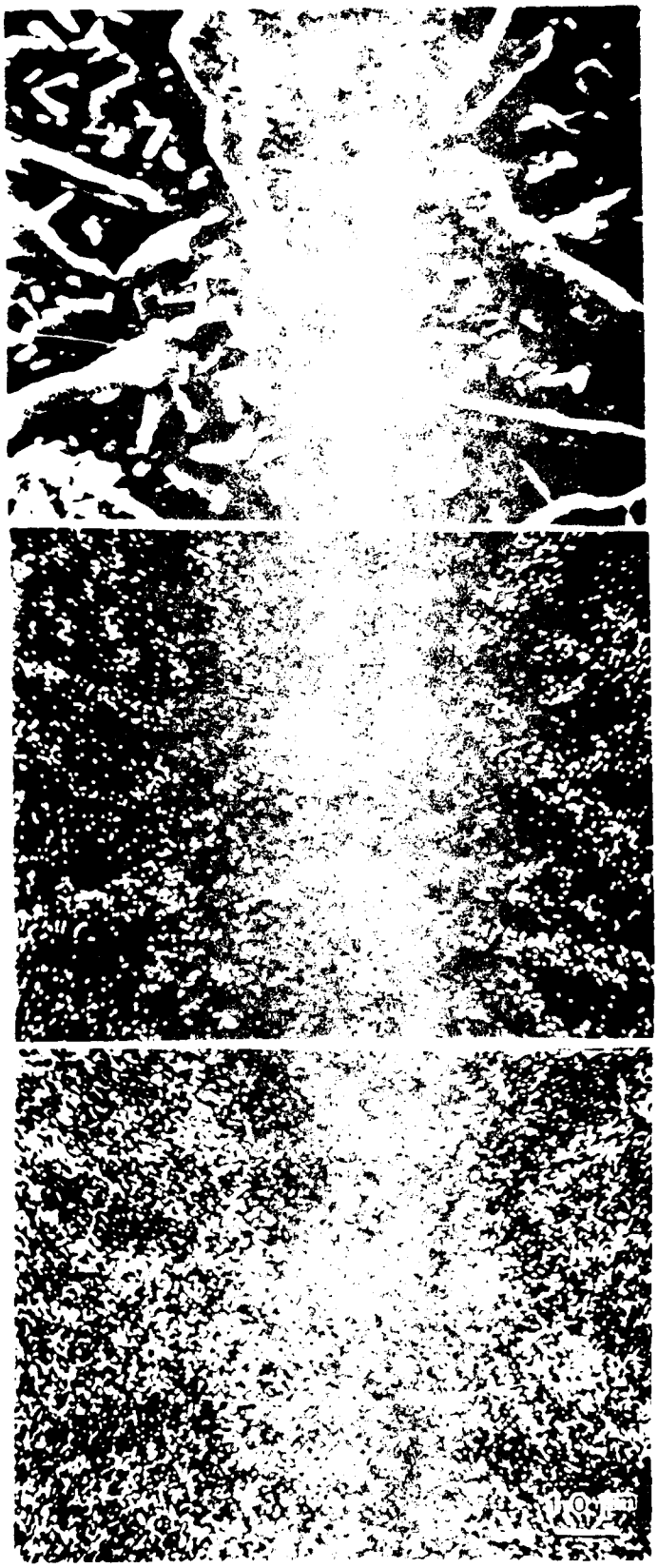

Fig. 2. SEM micrograph and [illegible] at 1450°C for 3 hr:
(a) SEM, (b) [illegible]

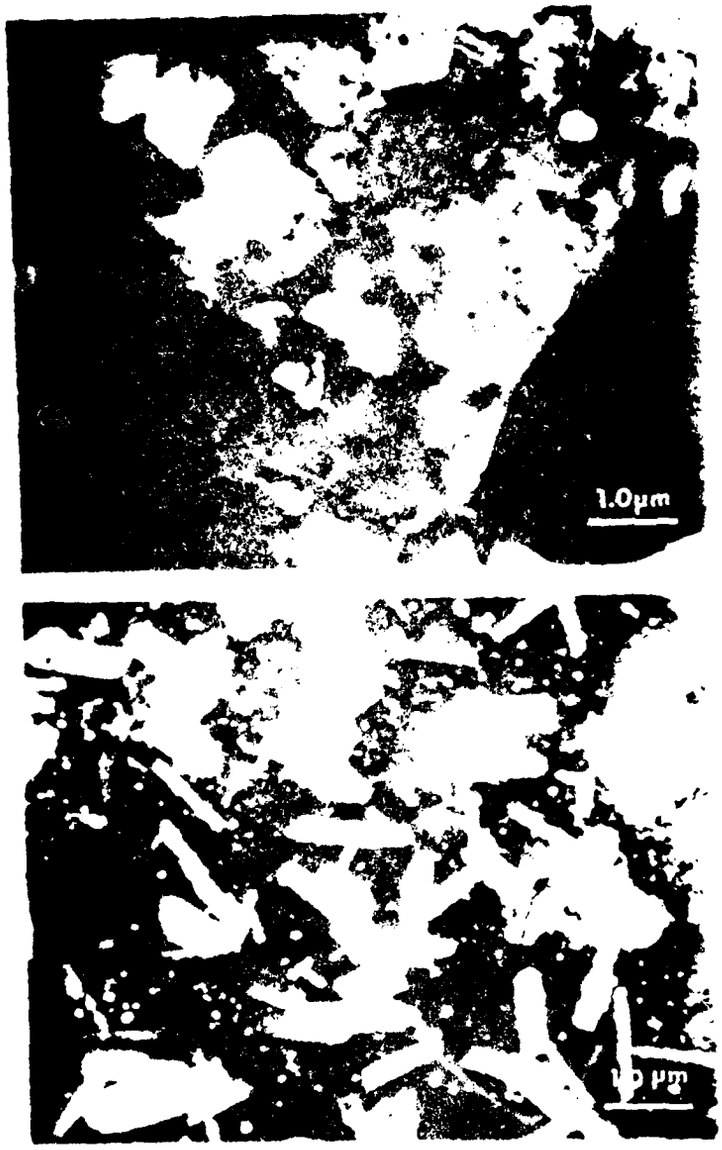

Fig. 3. [illegible] electron image [illegible] at 1450°C for [illegible]

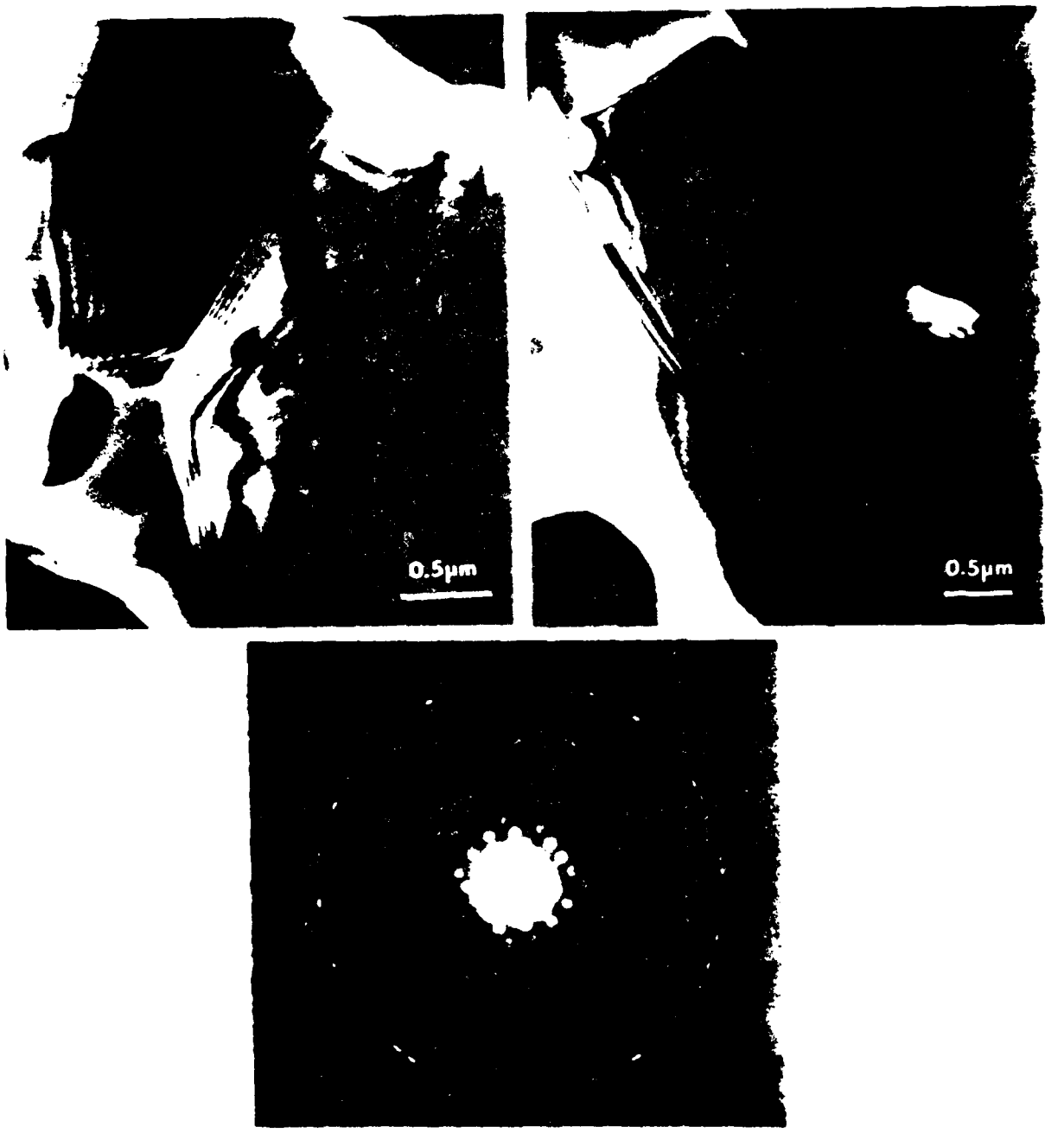

Fig. 4. DF TEM micrograph [illegible] and a stacking fault (a), and [illegible] beam diffraction pattern with [illegible]

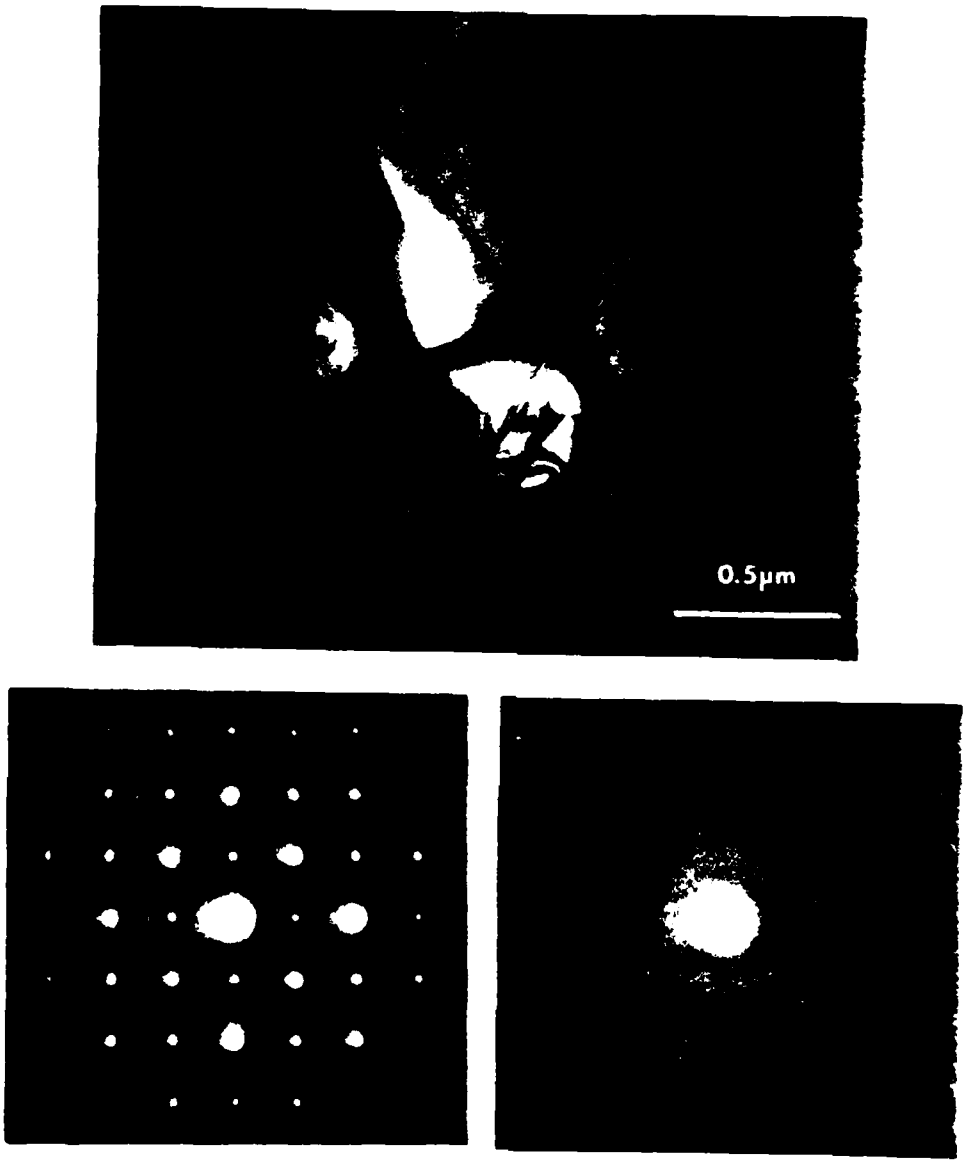

Fig. 5. BF TEM micrograph of SiO_2 phase (a); diffraction patterns from this phase (b) and from grain boundary phase (c).

Fig. 6. BF TEM micrograph of back-thinned specimen oxidized at 1000°C for 20 hr.

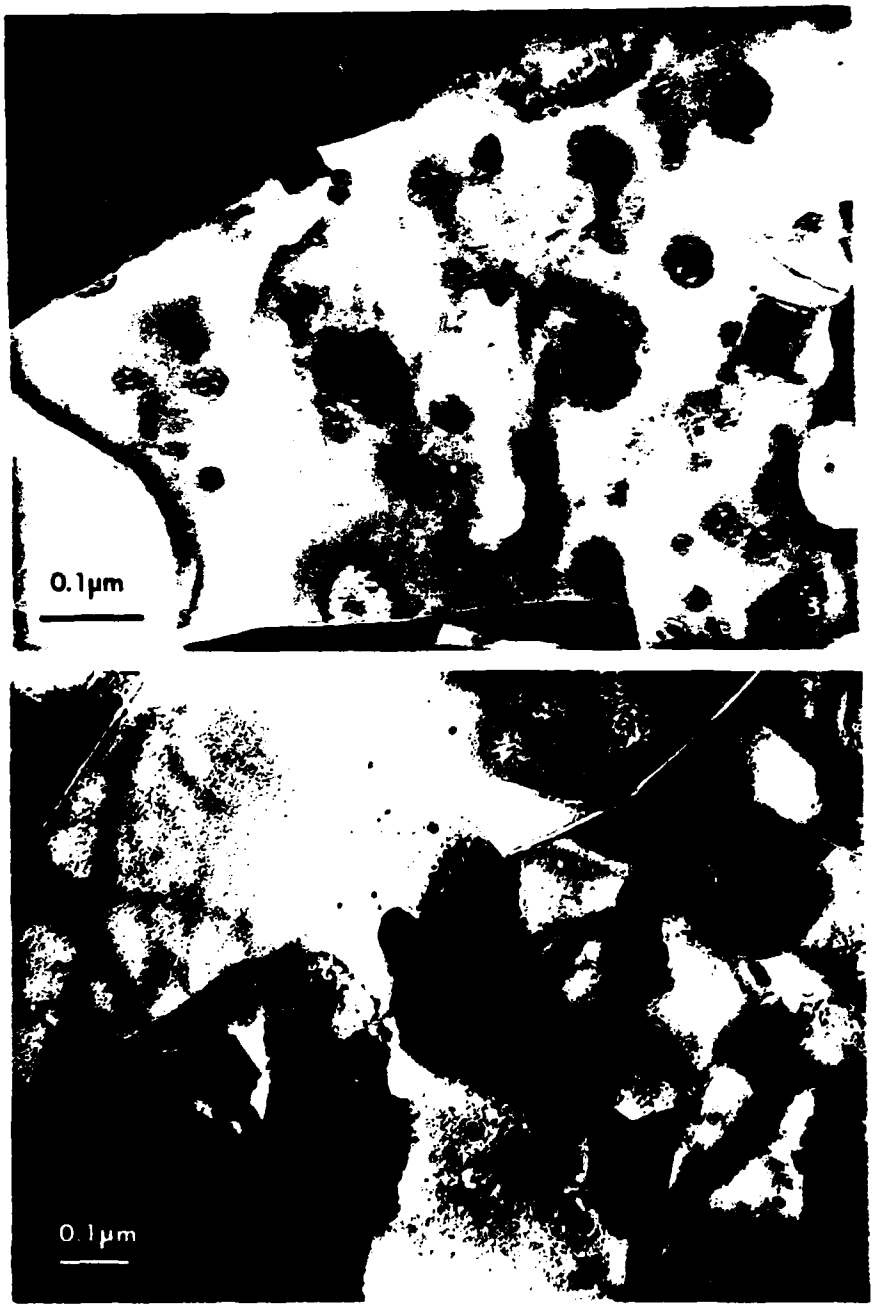

Fig. 7. BF TEM micrographs of specimens ion-milled and then oxidized at 1000°C for 2 hrs.

FILMED

7-8